International Journal of Nanomedicine

Dovepress
Taylor & Francis Group

Open Access Full Text Article

ORIGINAL RESEARCH

Stimuli-Responsive Nodal Dual-Drug Polymer Nanoparticles for Cancer Therapy

Gaizhen Kuang[1,2], Jiaze Ding[1,2], Weiyi Xie[1,2], Zihui Ye[1,2], Qingfei Zhang[1,2]

[1]The First Affiliated Hospital, Wenzhou Medical University, Wenzhou, Zhejiang, People's Republic of China; [2]School of Basic Medical Sciences, Wenzhou Medical University, Wenzhou, Zhejiang, People's Republic of China

Correspondence: Gaizhen Kuang; Qingfei Zhang, Wenzhou Medical University, Wenzhou, Zhejiang, 325000, People's Republic of China, Email gzhkuang@wmu.edu.cn; 654626160@qq.com

Background: Polymeric drug delivery systems (DDSs) have gained significant attention in cancer therapy. However, these systems often respond to a single biological stimulus in tumor tissues or cells, limiting their effectiveness. While multi-sensitive DDSs improve therapeutic precision, their complex synthesis involving multi-step modifications remains challenging. Developing functionally integrated and simplified multiple stimuli-responsive DDSs is crucial to addressing tumor diversity and enhancing treatment efficacy.
Methods and Results: Here, we develop a dual-sensitive nodal dual-drug polymer nanoparticle (DDPoly NP) system for cancer therapy. This system combines a platinum(IV) prodrug (Cisplatin(IV)) with Demehylcantharidin (DMC) to create a dual-drug molecule (DDM). Then DDM is conjugated with methoxypolyethylene glycol (MPEG), forming a nodal dual-drug polymer (DDPoly). The amphiphilic polymer is capable of self-assembling into nanoparticles (DDPoly NPs) when in aqueous solution. The drug release experiments displayed that lower pH and reductive conditions simulating tumor microenvironment promoted the release of Cisplatin and DMC. Cytotoxicity studies demonstrated that DDPoly NPs exhibited superior anti-cancer activity compared to the single-drug system (SDPoly NPs). The IC_{50} values of DDPoly NPs against A549 cells (15.37 μM) and HeLa cells (17.05 μM) were significantly lower than those observed for SDPoly NPs, which were 40.48 μM for A549 cells and 38.11 μM for HeLa cells, respectively.
Conclusion: The study developed dual stimuli-responsive DDPoly NPs based on acid- and reduction-sensitive DDM, enabling tumor-specific activation without additional responsive components. DDPoly NPs triggered Pt(II) release via reduction and generated DMC through acid hydrolysis. The synergistic effect of DDPoly NPs lies in that DMC could inhibit the expression of serine/threonine protein phosphatase 2A (PP2A) and further elevate the expression of hyper-phosphorylated Akt (pAKt), thus blocking DNA repair to enhance Pt(II)-induced apoptosis. DDPoly NPs showed enhanced anti-cancer efficacy against cancer cells compared to SDPoly NPs, highlighting its potential for nanomedicine development.

Keywords: platinum drug, cancer therapy, chemotherapy, polymer nanoparticle, stimuli-responsive

Introduction

In recent decades, polymer-based drug delivery systems (DDSs) have garnered significant interest owing to their enhanced pharmacokinetics and superior tumor accumulation characteristics.[1–4] Significant efforts have been dedicated to creating controlled DDSs that respond to the microenvironments of tumor tissues or cells to enhance drug accumulation in tumor sites.[5,6] Biological stimuli typically utilized include pH, reductive potential, enzymes, oxidative stress, etc.[7,8] Among them, pH and redox stimuli are frequently used to initiate drug release from DDSs.[9–11] Under normal physiological conditions, the extracellular environment maintains a pH of approximately 7.4 and glutathione (GSH) concentrations between 2.0 to 20 μM. In contrast, tumor tissues and cells exhibit a more acidic extracellular microenvironment, with pH values typically ranging from 6.5 to 7.0. Intracellular GSH levels in tumors are markedly elevated, reaching approximately 0.5 to 10 mM.[12,13] Recently, numerous stimulus-responsive polymer DDSs have been documented for application in cancer therapy.[1,14] Despite their promise, several challenges persist. Polymeric DDSs are typically engineered to respond to a singular type of stimulus.[15] It is well-established that tumors represent complex systems, characterized by significant heterogeneity among tumor cells.[16] Consequently, polymeric DDSs that are responsive to a single stimulus could not effectively release their payload, potentially

Received: 6 February 2025
Accepted: 15 April 2025
Published: 23 April 2025

resulting in diminished therapeutic efficacy. Multi-sensitive polymeric DDSs, capable of facilitating controlled drug release and achieving superior therapeutic outcomes, have garnered significant attention in the scientific community.[17] However, the process typically necessitates intricate devise and synthesis, meticulous protection and deprotection steps, or post-polymerization modifications.[18] Thus, developing functional polymeric DDSs through ingenious design and straightforward synthesis continues to present a significant challenge.

Recently, platinum(IV) (Pt(IV)) complexes have been strategically utilized as prodrugs in the development of stimulus-responsive drug delivery systems.[2,19] This is attributed to their chemically modified properties and their ability to convert into highly cytotoxic platinum(II) (Pt(II)) species under reductive conditions or upon exposure to light irradiation.[20] Although there is great progress, challenges such as uncontrollable composition, unavoidable carrier material toxicity, and inconsistent drug loading still pose major issues, making the current state of precision therapeutics unsatisfactory.[21–23] In addition, the effect of single-agent chemotherapy is limited and often unsatisfactory. It has been established that Demethylcantharidin (DMC), an inhibitor of serine/threonine protein phosphatase 2A (PP2A), has been shown to augment the effectiveness of platinum-based chemotherapeutic agents.[24,25] Studies have demonstrated that an optimized synergistic chemotherapeutic effect is achieved with a Pt(II) to DMC ratio of 1:2.[26,27] Besides, the β-carboxylic amide group in DMC is acid-sensitively.[28,29] Thus, it is anticipated to design a dual-sensitive drug delivery system utilizing a Pt(IV) prodrug in conjunction with DMC to achieve the desired functionalities for synergistic tumor therapy.

Herein, we developed stimuli-responsive nodal dual-drug polymer nanoparticles (DDPoly NPs) for cancer therapy, as illustrated in Figure 1. DMC was initially conjugated with a cisplatin prodrug (Cisplatin(IV)) to form a dual-drug molecule (DDM), maintaining a stoichiometric ratio of platinum to DCM of 1:2. Following the conjugation of DDM with

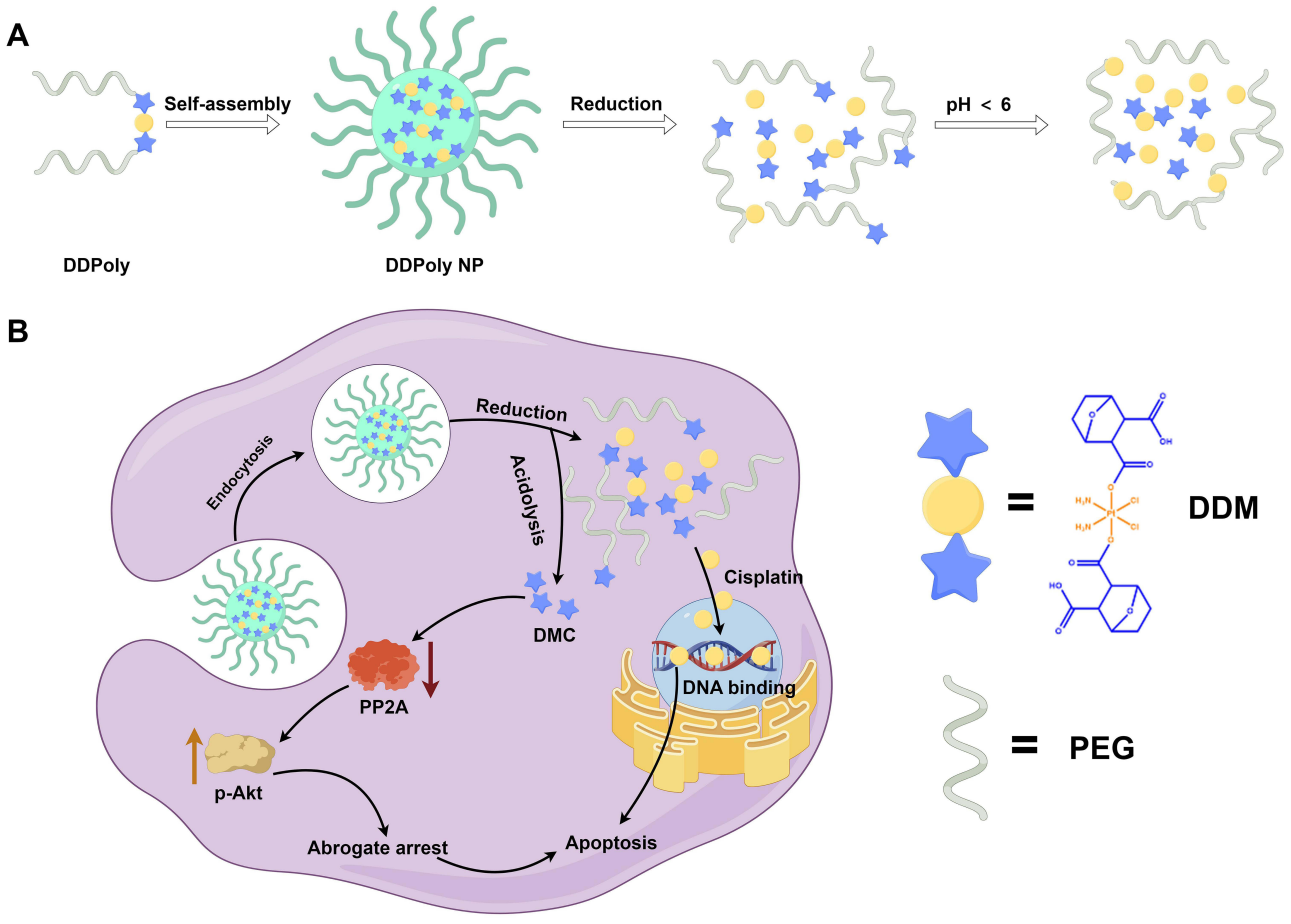

Figure 1 Schematic illustration of nodal dual-drug polymer nanoparticles (DDPoly NPs) for synergistic therapy. (**A**) Illustration of structure and self-assembly of DDPoly, and dual stimuli-responsive degradation of DDPoly NPs. (**B**) Anti-cancer mechanisms of DDPoly NPs after endocytosis by cancer cells. The schematic diagram was generated by Figdraw.

methoxypolyethylene glycol (MPEG), a nodal dual-drug polymer (DDPoly) was synthesized. As a contrast, succinic anhydride (SA) instead of DMC was conjugated with Cisplatin(IV) to obtain a single-drug molecule (SDM), which was further reacted with MPEG to get a nodal single-drug polymer (SDPoly). These two polymers could self-assemble into nanoparticles (SDPoly NPs, DDPoly NPs) in aqueous solution. After the endocytosis of the NPs by cancer cells, the drug node in the polymers undergoes cleavage in a reductive environment. Subsequently, the CisplatinPt(IV) located in the core of the NPs is reduced, leading to the release of the active Pt(II), which in turn causes DNA damage. Compared with SDPoly NPs, DDPoly NPs contain DMC in the node DDM. DMC was released within the acidic endo/lysosomal microenvironment and could inhibit PP2A, thereby obstructing the repair of damaged DNA and playing synergistic effects in chemotherapy. Thus, DDPoly NPs displayed better anti-cancer activities than SDPoly NPs.

Currently, dual-drug delivery nano-systems demonstrate significant potential in anti-tumor therapy, yet they still face critical limitations and challenges. The synergistic effects of dual-drug combinations are highly dependent on precise drug ratios.[27,30] However, variations in the physicochemical properties of distinct drugs, such as solubility and molecular weight, result in differential binding affinities of nanocarriers.[31,32] This disparity can lead to imbalanced drug loading and release ratios, thereby potentially compromising therapeutic efficacy. Besides, drug loading strategies relying on physical encapsulation or adsorption are prone to drug leakage or premature release during systemic circulation.[33,34] In addition, the preparation of dual-drug systems requires carrier material selection, functional modifications, etc., resulting in high process complexity and challenges in achieving large-scale production.[20,35] Moreover, certain nanomaterials (eg, inorganic nanoparticles) may exhibit biocompatibility concerns, with potential risks of immune responses or organ accumulation toxicity during prolonged use. In contrast, the designed DDPoly NPs system exhibits many advantages. The ratio of the two prodrugs was meticulously calibrated to enhance synergistic effects. DDPoly NPs feature concise and clear material types, straightforward preparation processes, and good stability. The degradation of DDPoly nanoparticles was specific to the tumor microenvironment, thereby enabling the release of both active Pt(II) and DMC at the tumor site, without necessitating additional stimulus-responsive molecules. These features render the DDPoly NP system a promising therapeutic formulation for cancer treatment.

Materials and Methods

Materials and Cell Lines

Cisplatin, Demehylcantharidin (DMC), methoxypolyethylene glycol amine (M_n = 2000 Da, $MPEG_{2k}$-NH_2), N-Hydroxysuccinimide (NHS), N-(3-Dimethylaminopropyl)-N′-ethylcarbodiimide hydrochloride (EDC·HCl), glutathione (GSH), and Succinic anhydride (SA) were bought from Macklin. Cell Counting Kit-8 (CCK8) and 4′,6-diamidino-2-phenylindole (DAPI) were obtained from Beyotime Biotechnology. γH2AX antibody, hyper-phosphorylated Akt (p-Akt) antibody, and corresponding fluorescence-labeled second antibodies were obtained from Bioss. Malachite Green Phosphatase assay specific for PP2A activity was obtained from Invitrogen. Human non-small lung carcinoma cell line (A549 cells), human cervical carcinoma cell line (Hela cells), and mouse fibroblasts (L929 cells) were purchased from the Cell Bank of the Chinese Academy of Sciences, Shanghai.

Synthesis of Single Drug Molecule (SDM) and Dual Drug Molecule (DDM)

Briefly, Cisplatin was suspended in a 30% hydrogen peroxide solution (H_2O_2) at ambient temperature for a duration of 24 h in the absence of light, in order to synthesize the prodrug form of Cisplatin(IV), as outlined in prior studies.[27,36] Then, the Cisplatin(IV) (668 mg, 2.0 mmol) and SA (205 mg, 2.05 mmol) or DMC (245 mg, 2.05 mmol) were dissolved in DMSO (10 mL) before stirring at 60 °C for 24 h. The obtained SDM or DDM was precipitated in cold diethyl ether and subsequently washed with cold acetone and diethyl ether, and then dried under vacuum conditions. The platinum content within the SDM or DDM was quantified utilizing inductively coupled plasma optical emission spectroscopy (ICP-OES). Before measurement, SDM or DDM was treated with nitric acid and heated to degrade. Then the solution was stepwise added H_2O_2 and deionized water, respectively, to obtain clear solutions.

Synthesis of Single-Drug Polymer (SDPoly) and Dual-Drug Polymer (DDPoly)

EDC·HCl (191.7 mg, 1.0 mmol), NHS (115.1 mg, 1.0 mmol), and SDM (267 mg, 0.50 mmol) or DDM (335 mg, 0.5 mmol) were dissolved in dried DMF (5 mL) and stirred for 1 h. Then, $MPEG_{2k}$-NH_2 (2.0 g) was introduced into the reaction mixture and stirred at ambient temperature for an additional 24 h. The polymer solution was then incrementally added to diethyl ether, resulting in the formation of a precipitate, which was subsequently dried under vacuum conditions. The resulting yellow solid, either SDPoly or DDPoly, underwent dialysis (molecular weight cut-off (MwCO) = 3500) against deionized water and was ultimately subjected to lyophilization.

Preparation of Single-Drug Polymer Nanoparticles (SDPoly NPs) and Dual-Drug Polymer Nanoparticles (DDPoly NPs)

SDPoly (20 mg) or DDPoly (20 mg) was initially dissolved in dimethyl sulfoxide (DMSO, 2 mL), followed by the gradual addition of water (20 mL) under continuous stirring to form the micellar nanoparticles (NPs). The resulting solution underwent dialysis against deionized water for three days and was subsequently subjected to freeze-drying. The size and morphology of the resulting SDPoly NPs or DDPoly NPs were characterized using dynamic light scattering (DLS) and transmission electron microscopy (TEM). The platinum content of SDPoly NPs or DDPoly NPs was determined by ICP-OES.

Stimuli-Responsiveness and Drug Release of SDPoly NPs and DDPoly NPs

Lyophilized SDPoly NPs or DDPoly NPs (4 mg) were dissolved in water (1 mL) with and without GSH (10 mM), respectively. After preparation, the solution was adjusted to either pH 7.4 or pH 5.0 before being transferred into an end-sealed dialysis bag (MwCO = 500). This dialysis bag was then submerged in 19 mL of the corresponding dialysis medium. The drug release system was maintained under incubation in a continuous shaker at a temperature of 37 °C. At specified time intervals, 1 mL of the dialysate was withdrawn and substituted with an equivalent volume of fresh solution. The concentration of platinum released from the NPs was quantified using ICP-OES. After the NPs incubated with different conditions for 48 h, the size and morphology of them were measured by DLS and TEM. The release of DMC was determined through an indirect analytical method. 200 μL of the above release medium at 48 h was used to inhibit the activity of PP2A, which was quantified using a specific PP2A assay kit. The relative activity of PP2A was calculated using the formula: PP2A activity = (mean absorbance of sample / mean absorbance of control) × 100%.

Cellular Uptake

To observe the cellular uptake behavior, SDPoly NPs or DDPoly NPs were firstly loaded with Nile red (NR) to obtain the NR-labelled NPs (SDPoly@NR NPs or DDPoly@NR NPs). Thereafter, SDPoly@NR NPs or DDPoly@NR NPs were added to 6-well plates containing A549 cells and incubated for 0.5 h or 4 h. After that, the cells were subjected to three washes with PBS, stained with 4′,6-diamidino-2-phenylindole (DAPI), and subsequently examined using confocal laser scanning microscopy (CLSM) or analyzed by flow cytometry.

Anti-Cancer Efficacy Evaluation

Cytotoxicity was evaluated utilizing a conventional CCK-8 assay. A549 and HeLa cells were plated in 96-well plates for an overnight period. Subsequently, the medium was replaced with DMC, DDM, SDM, SDPoly NPs, and DDPoly NPs, achieving a final platinum concentration ranging from 1.56 to 100 μM. Following a 48-hour incubation period, CCK-8 reagent was introduced into each well and incubated for an additional 1.5 h prior to measurement using a microplate reader at 450 nm.

For detecting the DNA damage, A549 cells were incubated with DMC (40 μM), SDPoly NPs (platinum concentration of 20 μM), or DDPoly NPs (platinum concentration of 20 μM) for 48 h. Subsequently, the cells were fixed and incubated with primary antibodies against γH2AX at 4 °C overnight. Then, the cells were visualized by CLSM after incubation with the fluorescent secondary antibody.

For the immunofluorescence staining procedure, A549 cells were incubated with SDPoly NPs and DDPoly NPs, each containing a platinum concentration of 20 μM, for 48 h. Subsequently, the cells were fixed and incubated with primary antibodies against p-Akt at 4 °C overnight. To facilitate visualization of the protein staining, the cells were subsequently treated with a secondary antibody conjugated to Alexa Fluor 488.

To assess toxicity to normal cells, L929 cells were plated in 96-well plates for an overnight period. Subsequently, the medium was replaced with SDPoly NPs or DDPoly NPs, achieving a final platinum concentration ranging from 1.56 to 100 μM. Following a 48-hour incubation period, the CCK-8 assay was conducted as above.

Statistical Analysis

All statistical data are expressed as the mean ± SD. Statistical significance was calculated via unpaired Student's *t*-tests. n.s.: no significance. * $p < 0.05$, ** $p < 0.01$, *** $p < 0.001$.

Results and Discussion

Firstly, the stimuli-responsive single drug molecule (SDM) and dual drug molecule (DDM) were synthesized according to the steps shown in Figure S1. Cisplatin was first oxidized by H_2O_2 to obtain Cisplatin(IV), which was further reacted with SA or DMC to generate SDM or DDM. The synthesis of SDM and DDM was successfully validated through proton nuclear magnetic resonance (^{1}H NMR), electrospray ionization mass spectrometry (ESI-MS), and ICP-OES. As shown in Figure 2A, the characteristic chemical shifts belonging to -NH_3 (c, 6.49 ppm), -CH_2-CH_2- (a, 2.48 ppm, and b, 2.37 ppm), and -COOH (d, 12.04 ppm) from SDM could be evidently and accurately observed in the ^{1}H NMR. Similarly, characteristic chemical shifts belonging to -NH_3 (a, 6.18 ppm), -CH- (b, 2.96 ppm), -CH- (c, 4.60 ppm, 4.70 ppm), and -CH_2- (d, 1.49 ppm) from DDM could also be detected (Figure 2B). The molecular ion peaks (m/z) at 532.0 and 669.0 belong to SDM and DDM, respectively, consistent with the theoretical values (Figure 2C and D). The Pt contents

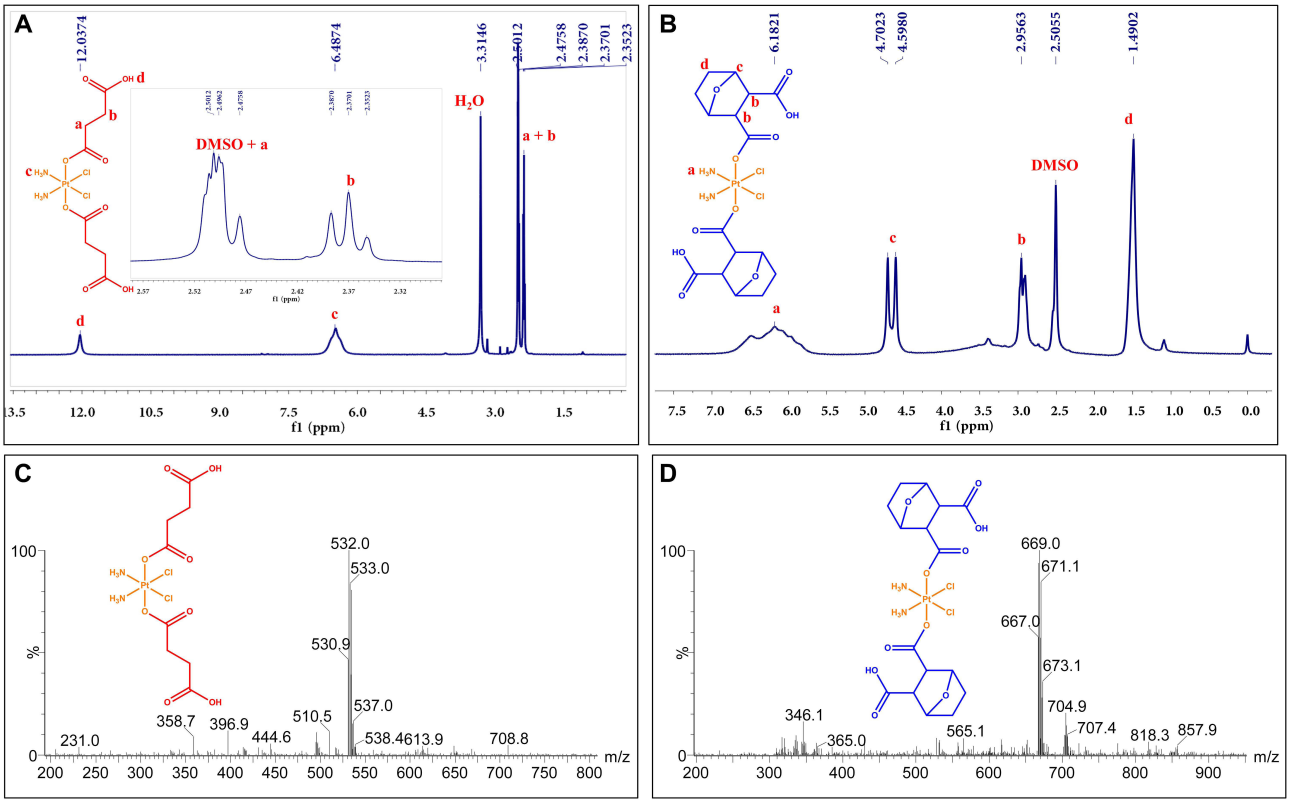

Figure 2 (**A**) ^{1}H NMR spectrum of the single-drug molecule (SDM) in DMSO-*d6*. δ (ppm): 2.48 and 2.37 (a and b, -CH_2-CH_2-), 6.49 (c, -NH_3), and 12.04 (d, -COOH). (**B**) ^{1}H NMR spectrum of the dual-drug molecule (DDM) in DMSO-*d6*. δ (ppm): 6.18 (a, -NH_3), 2.96 (b, -CH-), 4.60 and 4.70 (c, -CH-), and 1.49 (d, -CH-). (**C**) ESI-MS spectrum of SDM. (**D**) ESI-MS spectrum of DDM.

https://doi.org/10.2147/IJN.S517291

detected by ICP-OES were 36.43 wt% of SDM and 29.02 wt% of DDM, which are also consistent with the theoretical values (Table S1). Collectively, these results indicated the successful synthesis of SDM and DDM.

Subsequently, nodal drug polymers were prepared as shown in Figure S1. Briefly, single-drug polymer (SDPoly) or dual-drug polymer (DDPoly) was generated from the amidation between SDM and $MPEG_{2k}$-NH_2 or DDM and $MPEG_{2k}$-NH_2. From the ^1H NMR measurement, the characteristic chemical shifts in the SDM and DDM were also shown in SDPoly and DDPoly, respectively (Figure 3A and B). Both the SDPoly and DDPoly had hydrophobic node molecules (SDM and DDM) and hydrophilic MPEG. Thus, in an aqueous solution, the amphiphilic SDPoly and DDPoly could spontaneously assemble into corresponding nanoparticles (NPs). After the formation of SDPoly NPs and DDPoly NPs, the characteristic chemical shifts of SDM and DDM disappear in D_2O (Figure 3C and D). This phenomenon is attributed to their encapsulation within the core of the NPs.

The self-assembly processes of SDPoly NPs and DDPoly NPs are shown in Figure 4A and D, and the successful preparations of NPs were further verified by transmission electron microscopy (TEM) and dynamic light scattering (DLS) measurements. As shown in Figure 4B and E, both SDPoly NPs and DDPoly NPs displayed spherical micelle morphology. The diameters of SDPoly NPs and DDPoly NPs were 142 ± 10 nm and 143 ± 10 nm, respectively (Figure 4C and F). The Pt contents of SDPoly NPs and DDPoly NPs were detected and determined to be 4.11 wt% and 4.01 wt%, respectively (Table S1). Besides, the diameters of SDPoly NPs and DDPoly NPs showed no significant changes within 48 h when incubated in water, indicating the stability of these nanoparticles (Figure S2).

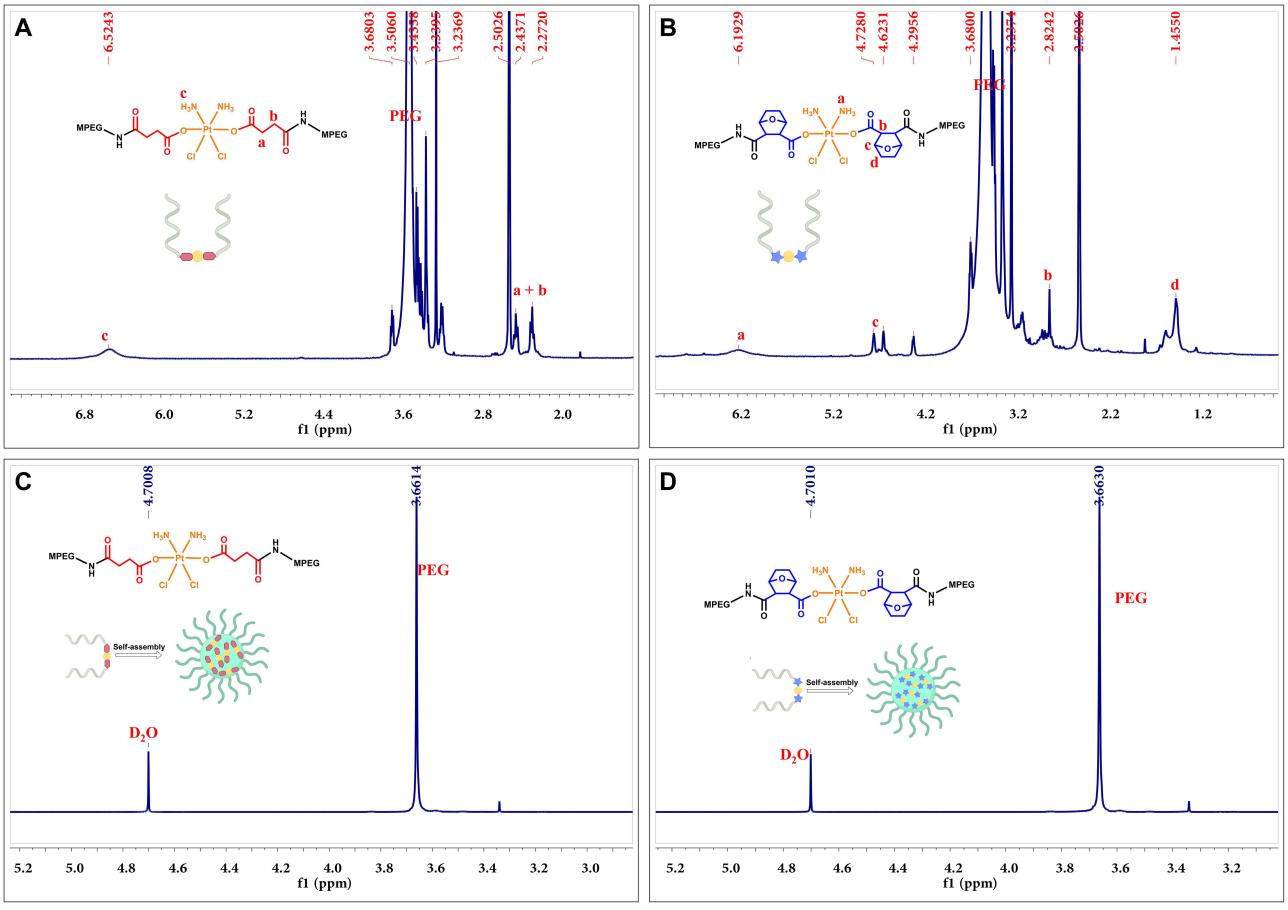

Figure 3 (**A**) ^1H NMR spectrum of the nodal single-drug polymer (SDPoly) in DMSO-*d6*. δ (ppm): 2.43 and 2.27 (a and b, -CH_2-CH_2-), 6.52 (c, -NH_3), and 3.68–3.43 (PEG). (**B**) ^1H NMR spectrum of the nodal dual-drug polymer (DDPoly) in DMSO-*d6*. δ (ppm): 6.19 (a, -NH_3), 2.82 (b, -CH-), 4.62 and 4.73 (c, -CH-), 1.46 (d, -CH-), and 3.68–3.40 (PEG). (**C**) ^1H NMR spectrum of the nodal single-drug polymer nanoparticles (SDPoly NPs) in D_2O. δ (ppm): 3.66 (PEG). (**D**) ^1H NMR spectrum of the nodal single-drug polymer nanoparticles (DDPoly NPs) in D_2O. δ (ppm): 3.66 (PEG).

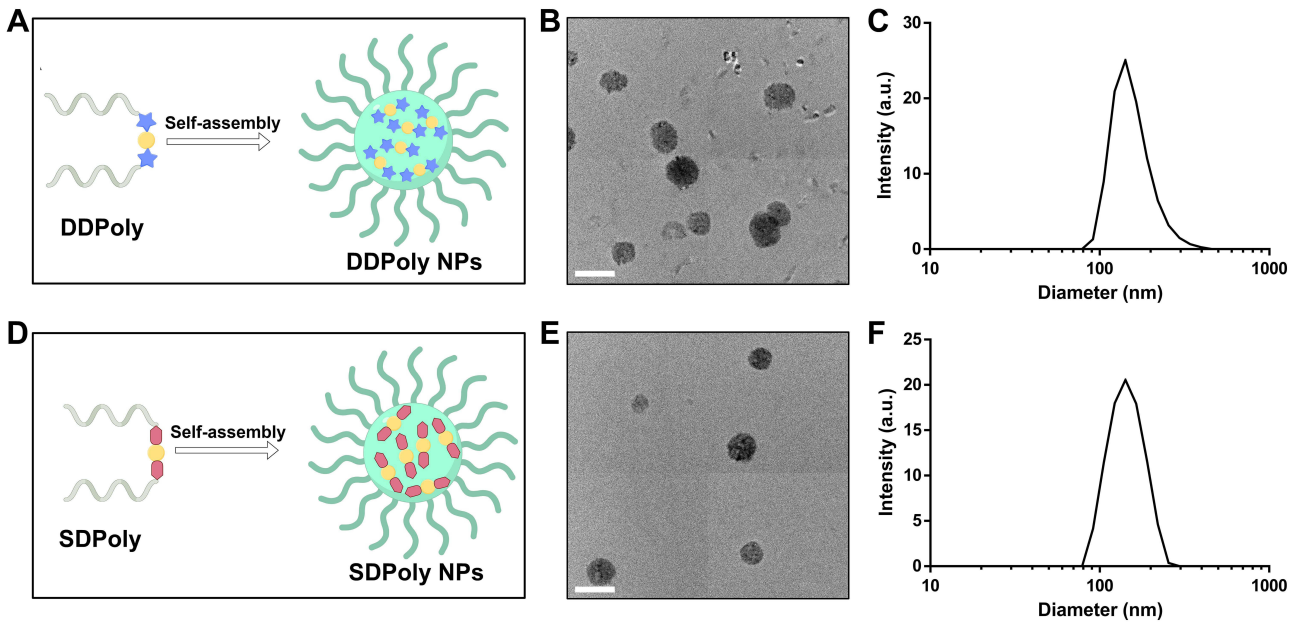

Figure 4 (**A**–**C**) Self-assembly process (**A**), TEM image (**B**), and size distribution (**C**) of DDPoly NPs. (**D**–**F**) Self-assembly process (**D**), TEM image (**E**), and size distribution (**F**) of SDPoly NPs. The scale bars are 200 nm.

Pt(IV) prodrugs are recognized for their sensitivity to reduction, facilitating the release of cytotoxic Pt(II) species in the presence of sodium ascorbate and/or GSH, which are overexpressed in tumor cells.[37–39] Besides, the *β*-carboxylic amide group, conjugated with DMC on the polymer node, exhibits acid sensitivity and has the potential to facilitate drug release in response to the extracellular pH characteristic of tumor environments.[15,28,29] Figure 5A and D described the stimuli-responsive disintegration processes of DDPoly NPs and SDPoly NPs, respectively. The degradation mechanism of the NPs was shown in Figure S3. Then, the reduction and pH dual-sensitive release behaviors of DDPoly NPs from the nature of Cisplatin(IV) prodrug and DMC-conjugate were investigated. As expected, DDPoly NPs and SDPoly NPs demonstrated considerable stability at a pH of 7.4, with platinum (Pt) release not exceeding 17.5% and 15.7% after 48 h, respectively (Figure 5B and E). However, the cumulative release of Pt from DDPoly NPs significantly increased to 32.5% at pH 5.0, while the SDPoly NPs displayed a slight increase to 21.0% in 48 h. This is attributed to the acid-sensitive nodal DDM in the polymer of DDPoly NPs. With the addition of GSH, both DDPoly NPs and SDPoly NPs displayed evidently quick release of drugs due to the reduction of Cisplatin(IV) in the node of the polymers. The Pt released from DDPoly NPs and SDPoly NPs reached 60.3% and 45.9%, respectively, in 48 h when incubated in a solution at pH 7.4 and with 10 mM GSH. As the pH declined to 5.0 and with 10 mM GSH, more than 73.0% and 50.2% of Pt was released from DDPoly NPs and SDPoly NPs within the same timeframe, demonstrating that drug release from DDPoly NPs is sensitive to both pH and reductant conditions. The release of DMC from DDPoly NPs under various conditions in 48 h was evaluated indirectly through a PP2A activity assay, which involved the specific inhibition of pure PP2A. As demonstrated in Figure S4, the activity of PP2A showed a significant reduction when incubated with the release medium containing DMC. Importantly, the release medium obtained from DDPoly NPs at a pH of 5.0 resulted in greater inhibition of PP2A compared to that at a pH of 7.0. In addition, when the release medium from DDPoly NPs at pH 5.0 was incubated with GSH, the activity of PP2A was further decreased. This observation suggests an enhanced release of DMC in acidic and reductant conditions. As shown in Figure 5C and F, following a 48-hour treatment of DDPoly NPs and SDPoly NPs without GSH at pH 7.4, the DLS signal still maintains a single peak. Although initially characterized by a single peak, the DLS signal underwent a notable transformation to broad peaks following the incubation of NPs in an aqueous solution at pH 5.0. Furthermore, treatment with GSH at a pH of 5.0 resulted in the emergence of multiple broad peaks. After the degradation, DDPoly NPs and SDPoly NPs fell apart into pieces, as directly observed by TEM. Taken together, the results demonstrated that the nodal drug-containing polymer NPs had effective dual-responsiveness.

https://doi.org/10.2147/IJN.S517291

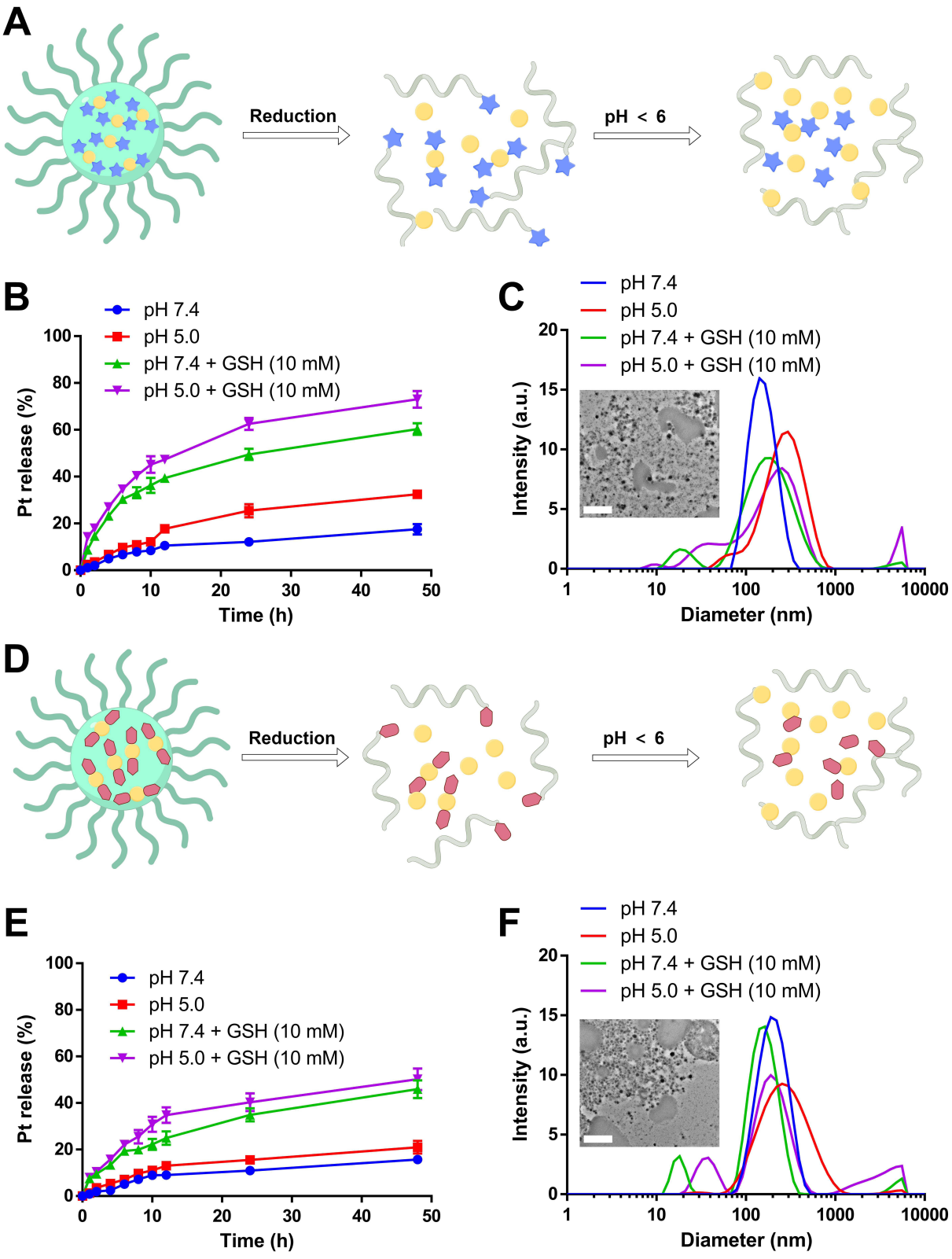

Figure 5 (**A**) Stimuli-responsive disassembly processes of DDPoly NPs. (**B**) Drug release profiles of DDPoly NPs after different treatments in 48 h. (**C**) Size distribution and morphology changes of DDPoly NPs after different treatments for 48 h. (**D**) Stimuli-responsive disassembly processes of SDPoly NPs. (**E**) Drug release profiles of SDPoly NPs after different treatments in 48 h. (**F**) Size distribution and morphology changes of SDPoly NPs after different treatments for 48 h. The inset TEM images are DDPoly NPs or SDPoly NPs after incubation with GSH at pH 5.0 for 48 h. The scale bars are 1 μm.

Then, the cellular internalization behaviors of DDPoly NPs and SDPoly NPs were studied. To facilitate the visualization of the internalization process, Nile red (NR) was employed as a fluorescent marker for loading into the NPs. Thus, the endocytosis of NR-labeled NPs (SDPoly@NR NPs and DDPoly@NR NPs) by cells could be observed through the fluorescence of NR. As shown in Figure 6A and B, in comparison to the control group, which indicated negligible red fluorescence, A549 cells treated with SDPoly@NR NPs or DDPoly@NR NPs exhibited a significant increase in red fluorescence intensity. With the prolonging of incubation time from 0.5 h to 4 h, more and more NPs were endocytosed demonstrated by more red fluorescence. Consistent results from the flow cytometry analysis indicated a notable increase in fluorescence intensity over time (Figure 6C and D). Following a 0.5-hour incubation period, the mean fluorescence intensities of SDPoly@NR NPs and DDPoly@NR NPs exhibited an increase of 3.85-fold and 3.99-fold, respectively, relative to the control group. After a 4-hour incubation, these intensities were further elevated, showing an increase of 13.56-fold and 13.53-fold, respectively.

Subsequently, the anti-cancer activity of DDPoly NPs and SDPoly NPs was investigated against non-small cell lung cancer A549 cells and cervical cancer Hela cells (Figure 7A and B). The small molecule drugs DMC, DDM, and SDM

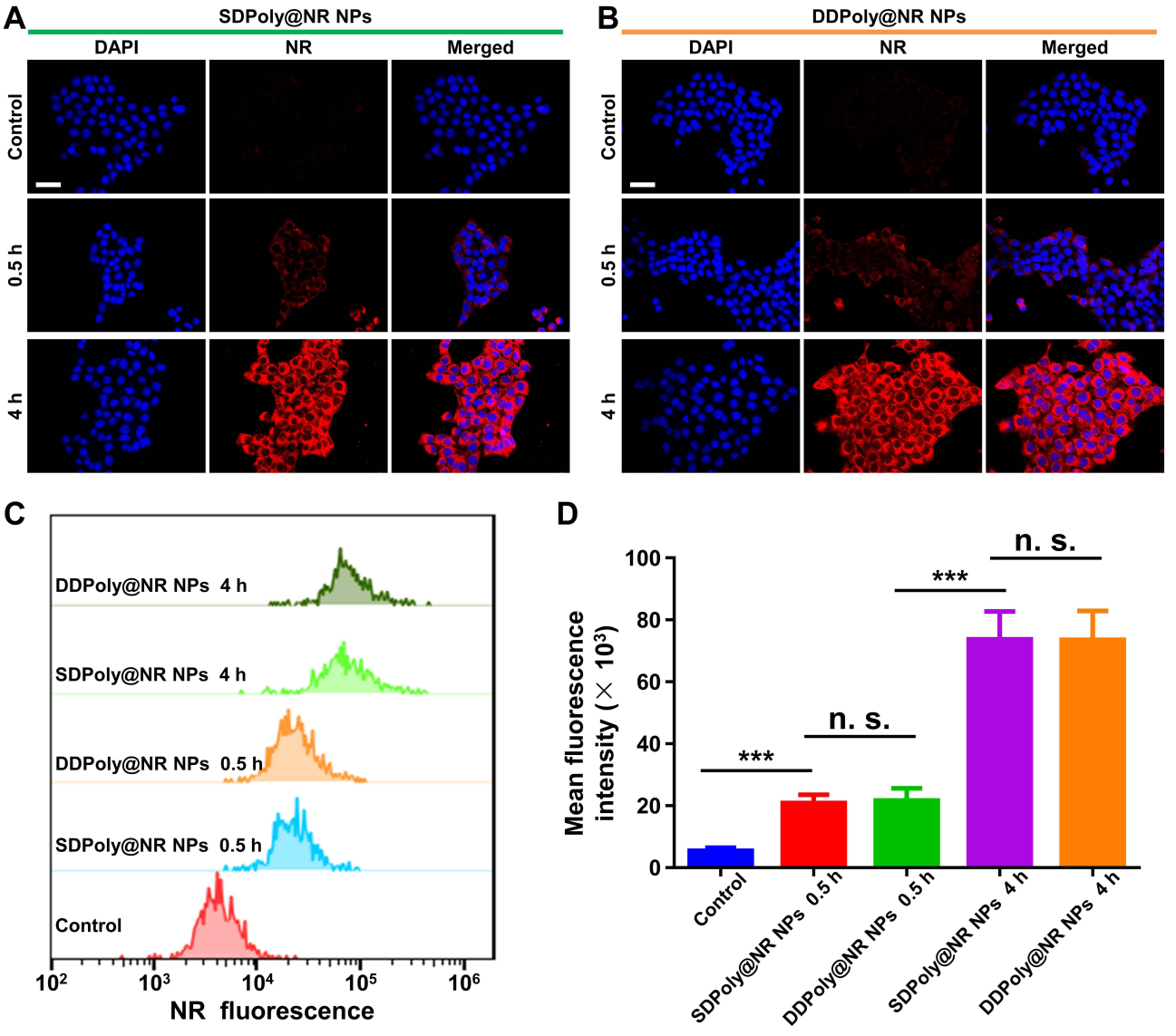

Figure 6 (**A** and **B**) CLSM images of A549 cells after incubation with SDPoly@NR NPs (**A**) or DDPoly@NR NPs (**B**) for 0.5 h or 4 h. The scale bars are 50 μm. (**C**) The cellular uptake analysis of SDPoly@NR NPs or DDPoly@NR NPs by flow cytometry. (**D**) The mean fluorescence intensity of cells incubated with SDPoly@NR NPs or DDPoly@NR NPs for different time intervals. n.s.: no significance. *** $p < 0.001$.

https://doi.org/10.2147/IJN.S517291

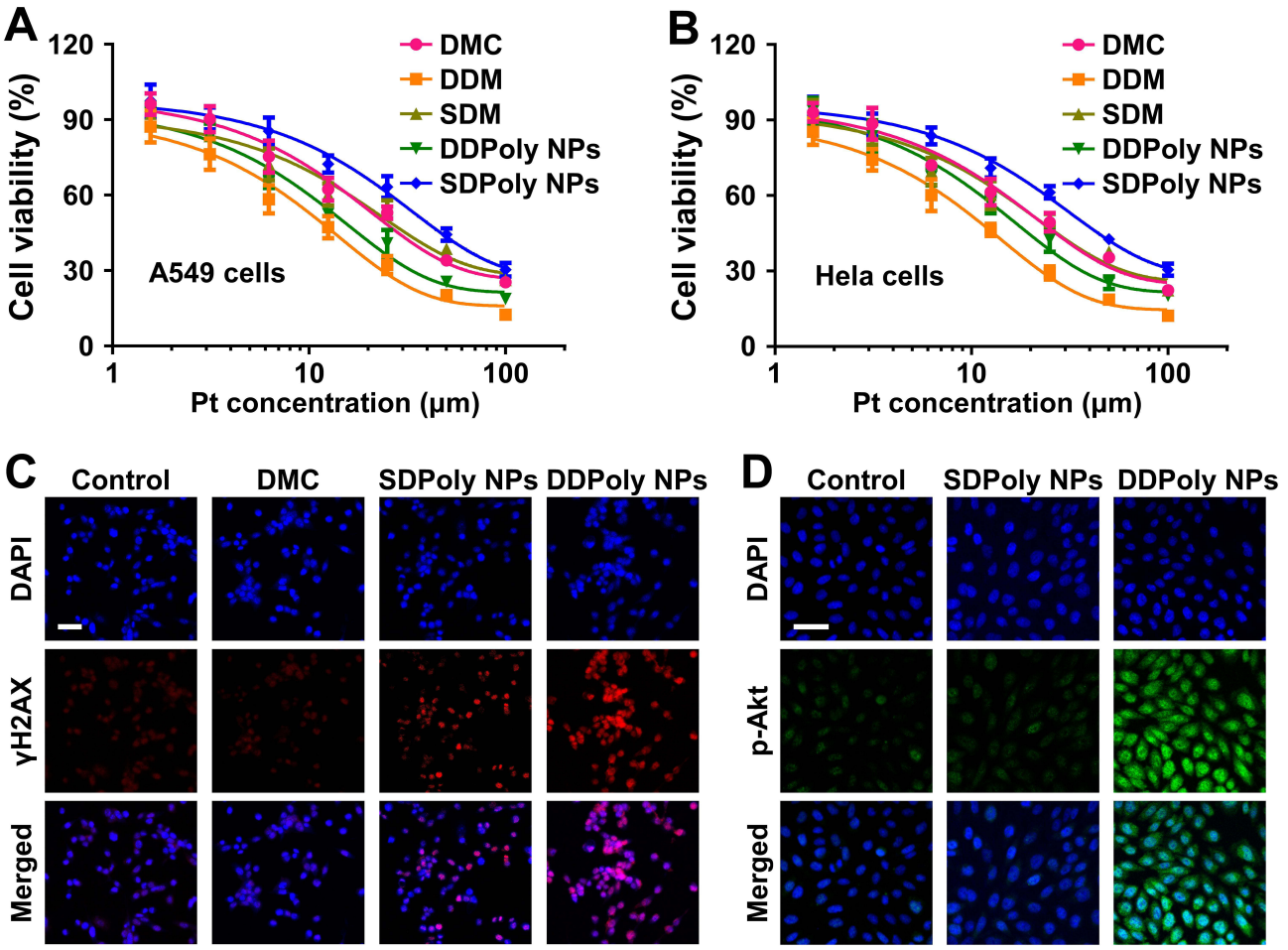

Figure 7 (**A** and **B**) Cell viability of A549 cells (**A**) and Hela cells (**B**) after treatment with different drugs for 48 h. (**C**) Immunofluorescent staining of γH2AX after treatment with different drugs for 48 h. The scale bars are 50 μm. (**D**) Immunofluorescent staining of p-Akt after treatment with different drugs for 48 h. The scale bars are 20 μm.

were employed as the comparison agents. For A549 cells, the IC_{50} values of DMC, DDM, and SDM were found to be 25.89 μM, 10.72 μM, and 26.26 μM, respectively, while for Hela cells, they were 23.41 μM, 10.12 μM, and 23.28 μM. The DDM and SDM had better cell-killing effects than their respective nanosystem of DDPoly NPs and SDPoly NPs, respectively. It could be attributed to the requirement for DDPoly NPs and SDPoly NPs to undergo endocytosis by the cells, followed by a gradual disassembly process. In addition, owing to the dual-stimuli dual-drug in the DDPoly NPs, the cytotoxicity of DDPoly NPs significantly increased when compared with SDPoly NPs. The IC_{50} values of DDPoly NPs against A549 cells (15.37 μM) and Hela cells (17.05 μM) were substantially lower than those of the SDPoly NPs against A549 cells (40.48 μM) and Hela cells (38.11 μM), respectively, confirming the synergistic action of DMC and the platinum drug. The results confirm that the nodal dual stimuli-responsive DDPoly NPs had better anticancer efficacy against cancers than SDPoly NPs.

Platinum-based drugs are widely employed as chemotherapeutic agents due to their capacity to induce DNA damage. To evaluate the DNA damage caused by the synthesized NPs, the DNA damage marker γH2AX was utilized. As illustrated in Figure 7C, the presence of the γH2AX marker was observed following the incubation of cells with DDPoly NPs and SDPoly NPs. The findings indicated that DDPoly NPs elicited the highest level of γH2AX expression in cells after a 24-hour treatment period, suggesting significant DNA damage. DMC is recognized as an inhibitor of PP2A, capable of obstructing the repair mechanisms of DNA damage induced by platinum-based chemotherapeutic agents. By inhibiting PP2A, DMC can activate the p-Akt signaling pathway. The resultant upregulation of p-Akt expression may lead to apoptosis due to the sustained progression of the cell cycle. To verify this, the expression level of p-Akt was

assessed following treatment with DDPoly NPs. As shown in Figure 7D, compared with the treatments of PBS and SDPoly NPs, DDPoly NPs significantly elevated the expression of p-Akt via the inhibition of PP2A. These findings suggest that the release of DMC from DDPoly NPs could modulate the expression of p-Akt. Besides, the cytotoxic effects of SDPoly NPs and DDPoly NPs on mouse fibroblast L929 cells were markedly diminished (Figure S5). This was attributable to the lack of low pH levels and high GSH concentrations, which significantly attenuated the activation of the NP systems. These results demonstrated that the developed stimuli-responsive systems exhibited high toxicity toward tumor cells while maintaining low toxicity toward normal cells.

Conclusion

In summary, we developed a DDPoly NP system for a dual stimuli-activatable synergistic chemotherapy approach. Based on the acid- and reduction-sensitive nodal dual-drug molecule (DDM), the fabrication of the system does not need additional stimulus-responsive molecules. The DDPoly NPs facilitated the reduction-triggered breakage of the Cisplatin(IV) prodrug, leading to the release of the active Pt(II) within tumor cells. Subsequently, the cleaved polymer segments were subjected to acid hydrolysis, resulting in the production of DMC. Notably, the synergistic cytotoxic efficacy of the Pt(II) and DMC within this platform was maintained at an optimum ratio of 1:2. The in vitro anti-cancer evaluation against non-small cell lung cancer A549 cells and cervical cancer Hela cells demonstrated that the DDPoly NPs had enhanced efficacy compared with the SDPoly NPs. The rational design of such dual-stimuli-responsive dual-drug delivery system holds promise for developing effective nanomedicine tailored to preclinical studies in non-small cell lung cancer, cervical cancer, etc., enhancing therapeutic synergy.

Acknowledgments

This research was supported by the National Natural Science Foundation of China under Grant No. 32201118 and the Zhejiang Provincial Natural Science Foundation of China under Grant No. LMS25H180007.

Disclosure

The author(s) report no conflicts of interest in this work.

References

1. Wei D, Sun Y, Zhu H, Fu Q. Stimuli-responsive polymer-based nanosystems for cancer theranostics. *ACS Nano*. 2023;17(23):23223–23261. doi:10.1021/acsnano.3c06019
2. Xiao H, Yan L, Dempsey EM, et al. Recent progress in polymer-based platinum drug delivery systems. *Prog Polym Sci*. 2018;87:70–106.
3. Torchilin V. Tumor delivery of macromolecular drugs based on the EPR effect. *Adv Drug Deliv Rev*. 2011;63(3):131–135. doi:10.1016/j.addr.2010.03.011
4. Fang J, Islam W, Maeda H. Exploiting the dynamics of the EPR effect and strategies to improve the therapeutic effects of nanomedicines by using EPR effect enhancers. *Adv Drug Deliv Rev*. 2020;157:142–160. doi:10.1016/j.addr.2020.06.005
5. Li X, Peng X, Zoulikha M, et al. Multifunctional nanoparticle-mediated combining therapy for human diseases. *Signal Transduct Target Ther*. 2024;9(1):1.
6. Jana D, Zhao Y. Strategies for enhancing cancer chemodynamic therapy performance. *Exploration*. 2022;2(2):20210238.
7. Peng H, Yao F, Zhao J, et al. Unraveling mitochondria-targeting reactive oxygen species modulation and their implementations in cancer therapy by nanomaterials. *Exploration*. 2023;3(2):20220115. doi:10.1002/EXP.20220115
8. Mura S, Nicolas J, Couvreur P. Stimuli-responsive nanocarriers for drug delivery. *Nat Mater*. 2013;12(11):991–1003. doi:10.1038/nmat3776
9. Ding H, Tan P, Fu S, et al. Preparation and application of pH-responsive drug delivery systems. *J Control Release*. 2022;348:206–238. doi:10.1016/j.jconrel.2022.05.056
10. Gu H, Mu S, Qiu G, et al. Redox-stimuli-responsive drug delivery systems with supramolecular ferrocenyl-containing polymers for controlled release. *Coord Chem Rev*. 2018;364:51–85. doi:10.1016/j.ccr.2018.03.013
11. Li X, Yue R, Guan G, Zhang C, Zhou Y, Song G. Recent development of pH-responsive theranostic nanoplatforms for magnetic resonance imaging-guided cancer therapy. *Exploration*. 2023;3(3):20220002. doi:10.1002/EXP.20220002
12. Chen B, Dai W, He B, et al. Current multistage drug delivery systems based on the tumor microenvironment. *Theranostics*. 2017;7(3):538–558. doi:10.7150/thno.16684
13. Bobko AA, Eubank TD, Voorhees JL, et al. In vivo monitoring of pH, redox status, and glutathione using L-band EPR for assessment of therapeutic effectiveness in solid tumors. *Magn Reson Med*. 2012;67(6):1827–1836. doi:10.1002/mrm.23196
14. Qiao Y, Wan J, Zhou L, et al. Stimuli-responsive nanotherapeutics for precision drug delivery and cancer therapy. *WIREs Nanomed Nanobiotech*. 2019;11(1):e1527. doi:10.1002/wnan.1527
15. Wu Y, Zhou D, Zhang Q, et al. Dual-sensitive charge-conversional polymeric prodrug for efficient codelivery of demethylcantharidin and doxorubicin. *Biomacromolecules*. 2016;17(8):2650–2661. doi:10.1021/acs.biomac.6b00705

16. Wang J, Sun X, Mao W, et al. Tumor redox heterogeneity-responsive prodrug nanocapsules for cancer chemotherapy. *Adv Mater*. 2013;25(27):3670–3676. doi:10.1002/adma.201300929
17. Cheng R, Meng F, Deng C, Klok H-A, Zhong Z. Dual and multi-stimuli responsive polymeric nanoparticles for programmed site-specific drug delivery. *Biomaterials*. 2013;34(14):3647–3657. doi:10.1016/j.biomaterials.2013.01.084
18. Han L, Tang C, Yin C. Dual-targeting and pH/redox-responsive multi-layered nanocomplexes for smart co-delivery of doxorubicin and siRNA. *Biomaterials*. 2015;60:42–52. doi:10.1016/j.biomaterials.2015.05.001
19. Yu Y, Xu Q, He S, et al. Recent advances in delivery of photosensitive metal-based drugs. *Coord Chem Rev*. 2019;387:154–179. doi:10.1016/j.ccr.2019.01.020
20. He S, Li C, Zhang Q, et al. Tailoring platinum(IV) amphiphiles for self-targeting all-in-one assemblies as precise multimodal theranostic nanomedicine. *ACS Nano*. 2018;12(7):7272–7281. doi:10.1021/acsnano.8b03476
21. Liu Y, Ai K, Ji X, et al. Comprehensive insights into the multi-antioxidative mechanisms of melanin nanoparticles and their application to protect brain from injury in ischemic stroke. *J Am Chem Soc*. 2017;139(2):856–862. doi:10.1021/jacs.6b11013
22. Zhong J, Li L, Zhu X, et al. A smart polymeric platform for multistage nucleus-targeted anticancer drug delivery. *Biomaterials*. 2015;65:43–55. doi:10.1016/j.biomaterials.2015.06.042
23. Pan L, Liu J, He Q, Shi J. MSN-mediated sequential vascular-to-cell nuclear-targeted drug delivery for efficient tumor regression. *Adv Mater*. 2014;26(39):6742–6748. doi:10.1002/adma.201402752
24. Lu J, Kovach JS, Johnson F, et al. Inhibition of serine/threonine phosphatase PP2A enhances cancer chemotherapy by blocking DNA damage induced defense mechanisms. *Proc Natl Acad Sci* 2009;106(28):11697–11702. doi:10.1073/pnas.0905930106
25. Zhou D, Cong Y, Qi Y, et al. Overcoming tumor resistance to cisplatin through micelle-mediated combination chemotherapy. *BiomateR Sci*. 2015;3(1):182–191. doi:10.1039/C4BM00305E
26. Zhou D, He S, Cong Y, et al. A polymer–(multifunctional single-drug) conjugate for combination therapy. *J Mater Chem B*. 2015;3(24):4913–4921. doi:10.1039/C5TB00576K
27. Cong Y, Xiao H, Xiong H, et al. Dual drug backboned shattering polymeric theranostic nanomedicine for synergistic eradication of patient-derived lung cancer. *Adv Mater*. 2018;30(11):1706220. doi:10.1002/adma.201706220
28. Lee Y, Fukushima S, Bae Y, Hiki S, Ishii T, Kataoka K. A protein nanocarrier from charge-conversion polymer in response to endosomal pH. *J Am Chem Soc*. 2007;129(17):5362–5363. doi:10.1021/ja071090b
29. Li L, Sun W, Zhong J, et al. Multistage nanovehicle delivery system based on stepwise size reduction and charge reversal for programmed nuclear targeting of systemically administered anticancer drugs. *AdV Funct Mater*. 2015;25(26):4101–4113. doi:10.1002/adfm.201501248
30. Tu Y, Zheng R, Yu F, Xiao X, Jiang M, Yuan Y. Dual drug delivery system with flexible and controllable drug ratios for synergistic chemotherapy. *Sci Chin Chem*. 2021;64(6):1020–1030. doi:10.1007/s11426-020-9964-x
31. Yang K, Yang Z, Yu G, Nie Z, Wang R, Chen X. Polyprodrug nanomedicines: an emerging paradigm for cancer therapy. *Adv Mater*. 2022;34(6):e2107434. doi:10.1002/adma.202107434
32. Dufort S, Sancey L, Coll J-L. Physico-chemical parameters that govern nanoparticles fate also dictate rules for their molecular evolution. *Adv Drug Deliv Rev*. 2012;64(2):179–189. doi:10.1016/j.addr.2011.09.009
33. Seidi F, Zhong Y, Xiao H, Jin Y, Crespy D. Degradable polyprodrugs: design and therapeutic efficiency. *Chem Soc Rev*. 2022;51(15):6652–6703. doi:10.1039/d2cs00099g
34. Wang N, Cheng X, Li N, Wang H, Chen H. Nanocarriers and their loading strategies. *Adv Healthcare Mater*. 2019;8(6):1801002. doi:10.1002/adhm.201801002
35. Wei X, Song M, Li W, Huang J, Yang G, Wang Y. Multifunctional nanoplatforms co-delivering combinatorial dual-drug for eliminating cancer multidrug resistance. *Theranostics*. 2021;11(13):6334. doi:10.7150/thno.59342
36. Zhang Q, Kuang G, He S, et al. Chain-shattering Pt(IV)-backboned polymeric nanoplatform for efficient CRISPR/Cas9 gene editing to enhance synergistic cancer therapy. *Nano Res*. 2021;14(3):601–610. doi:10.1007/s12274-020-3066-4
37. Wilson JJ, Lippard SJ. Synthetic methods for the preparation of platinum anticancer complexes. *Chem Rev*. 2014;114(8):4470–4495. doi:10.1021/cr4004314
38. Gao X, Lei G, Wang B, et al. Encapsulation of platinum prodrugs into PC7A polymeric nanoparticles combined with immune checkpoint inhibitors for therapeutically enhanced multimodal chemotherapy and immunotherapy by activation of the STING pathway. *Adv Sci*. 2023;10(4):2205241. doi:10.1002/advs.202205241
39. Wang Z, Wang N, Cheng S-C, et al. Phorbiplatin, a highly potent Pt (IV) antitumor prodrug that can be controllably activated by red light. *Chem*. 2019;5(12):3151–3165. doi:10.1016/j.chempr.2019.08.021